crystals

MDPI

Article

Synthesis, Crystal Structure, and Magnetic Properties of Amidate and Carboxylate Dimers of Ruthenium

Patricia Delgado-Martínez [1], Carlos Freire [1], Rodrigo González-Prieto [1], Reyes Jiménez-Aparicio [1,*], José L. Priego [1,*] and M. Rosario Torres [2]

[1] Departamento de Química Inorgánica, Facultad de Ciencias Químicas, Universidad Complutense de Madrid, Ciudad Universitaria, E-28040 Madrid, Spain; patriciadelgado@ucm.es (P.D.-M.); freisss22@gmail.com (C.F.); rodgonza@ucm.es (R.G.-P.)

[2] Centro de Asistencia a la Investigación Difracción Rayos X, Facultad de Ciencias Químicas, Universidad Complutense de Madrid, Ciudad Universitaria, E-28040 Madrid, Spain; mrtorres@quim.ucm.es

* Correspondence: reyesja@quim.ucm.es (R.J.-A.); bermejo@quim.ucm.es (J.L.P.)

Academic Editor: Shujun Zhang
Received: 15 June 2017; Accepted: 25 June 2017; Published: 27 June 2017

Abstract: Solvothermal and microwave-assisted methods have been used to prepare several amidate and carboxylate complexes of the type $[Ru_2X(\mu\text{-}NHOCC_6H_3\text{-}3,5\text{-}(OMe)_2)_4]_n$ [X = Cl (**1**), Br (**2**), I (**3**)] and $[Ru_2X(\mu\text{-}O_2CC_6H_3\text{-}3,5\text{-}(OMe)_2)_4]_n$ [X = Cl (**4**), Br (**5**), I (**6**)]. Complexes **4**–**6** have also been obtained by conventional synthesis which is ineffective to prepare the amidate compounds. However, single crystals of complexes **1**–**5** were obtained using the solvothermal method. The single crystal X-ray structure determination of compounds **1**–**5** have been carried out. All complexes display a paddlewheel-type structure with the metal atoms connected by four bridging amidate or carboxylate ligands. Chloride, bromide, or iodide anions connect the dimetallic units, producing one-dimensional zigzag chains. The magnetic properties of all compounds were studied. The magnetic moment at room temperature are in accordance with an electronic configuration with three unpaired electrons $\sigma^2\pi^4\delta^2(\pi^*\delta^*)^3$ per dimer unit. The fit of the magnetic data suggests the existence, in these complexes, of a weak antiferromagnetic intermolecular interaction between the diruthenium units mediated by the halide ligand and an appreciable zero-field splitting in the diruthenium moieties.

Keywords: diruthenium; multiple bonds; metal-metal bonds; microwave; solvothermal; amidates; carboxylates; magnetic properties

1. Introduction

The synthesis and reactivity of paddlewheel diruthenium complexes of the type $Ru_2Cl(\mu\text{-}L\text{-}L)_4$ (L-L = mononegative, three-atom donor ligand) have been intensively studied due to their interesting magnetic and electronic properties [1]. In these complexes, the L-L ligand bridge two multiply-bonded ruthenium atoms. The most studied compound of this type of paddlewheel complexes are the chloridotetracarboxylatodiruthenium(II,III) $[Ru_2Cl(\mu\text{-}O_2CR)_4]$ (R = alkyl or aryl) [2,3]. The usual method for obtaining these compounds is through a metathesis reaction of $[Ru_2Cl(\mu\text{-}O_2CMe)_4]$ with an excess of the corresponding carboxylic acid in a mixture of methanol/water (1:1) at reflux for several hours [4,5]. However, the interchange reaction of the acetate ligands by amidate groups to give the analogous $[Ru_2Cl(\mu\text{-}NHOCR)_4]$ cannot be carried out under mild reaction conditions [6–13]. Johnson and Powell [14] demonstrated some years ago that the microwave activation is useful to prepare dimolybdenum compounds in short periods of time and with good yields. More recently, the microwave activation and the solvothermal methods have proven to be as a very effective synthetic methods for the substitution process of acetate groups in $[Ru_2Cl(\mu\text{-}O_2CMe)_4]$ by N,N- or N,O-donor

ligands (N,N = triazenide, formamidinate or guanidinate; N,O = arylamidate) [15–18]. On the other hand, the solvothermal reactions are carried out in a closed system at relatively high temperature and pressure and in these conditions the compounds increase their solubility. As a consequence, the slow cooling of the reaction mixture frequently leads to single crystals. This is an important advantage in the preparation of the very insoluble tetraamidatodiruthenium complexes. Due to this low solubility the number of bromo- and iodotetraamidatodiruthenium(II,III) compounds are very scarce and only recently some examples have been prepared using solvothermal methods [18].

In this paper, we describe the preparation and crystal structure of three new amidate complexes $[Ru_2X(\mu\text{-}NHOCC_6H_3\text{-}3,5\text{-}(OMe)_2)_4]_n$ [X = Cl (**1**), Br (**2**), I (**3**)] using the 3,5-dimethoxybenzamidate ligand. The preparation and structure of two new carboxylates complexes with the analogous 3,5-dimethoxybenzoate ligand $[Ru_2X(\mu\text{-}O_2CC_6H_3\text{-}3,5\text{-}(OMe)_2)_4]_n$ [X = Cl (**4**), Br = (**5**)] are also described. The iodo derivative $[Ru_2I(\mu\text{-}O_2CC_6H_3\text{-}3,5\text{-}(OMe)_2)_4]_n$ (**6**) has been isolated as microcrystalline solid. We have used the 3,5-dimethoxybenzamidate ligand and their analogue carboxylate ligand in order to compare the properties of the amidato and carboxylato diruthenium derivatives.

2. Results and Discussion

2.1. Synthesis

The synthesis of the amidato complexes $[Ru_2X(\mu\text{-}NHOCC_6H_3\text{-}3,5\text{-}(OMe)_2)_4]_n$ [X = Cl (**1**), Br (**2**), I (**3**)], have been carried out by solvothermal and microwave assisted solvothermal methods. However, the thermal activation in solution does not produce the complexes as has been previously observed for analogous compounds [6–13]. To achieve the substitution of the carboxylate ligands in $[Ru_2X(\mu\text{-}O_2CMe)_4]_n$ (X = Cl, Br, I) by the corresponding amidate groups the presence of triethylamine and the corresponding halide salt (LiCl for **1**, KBr for **2** and KI for **3**) have been used in both methods [19]. In all cases the substitution of the acetate ligands leads to the tetraamidate complexes **1**–**3** in moderate yields (35–62%) except in the microwave synthesis for complex **2** (2%). The microwave activation leads to single-phase microcrystalline powders whereas the solvothermal synthesis allows the formation of high quality single crystals. As expected, the reaction times using microwave activation are shorter than used in the solvothermal synthesis.

The analogous tetracarboxylates $[Ru_2X(\mu\text{-}O_2CC_6H_3\text{-}3,5\text{-}(OMe)_2)_4]_n$ [X = Cl (**4**), Br (**5**), I (**6**)] have been obtained by the solvothermal and microwave assisted methods in good yields (59–90%). However, in contrast to the amidate complexes **1**–**3** the conventional metathesis reaction of $[Ru_2Cl(\mu\text{-}O_2CMe)_4]$ with the 3,5-dimethoxybenzoic acid in water/methanol (1:1) at reflux leads also to the formation of complexes **4**–**6** (yields: 43–80%). Thus, although the conventional method is useful to obtain these carboxylate complexes, the insolubility of compounds **4**–**6** prevents obtaining single crystals. However, the experimental conditions used in the solvothermal method led directly to the formation of single crystals in the case of complexes **4** and **5**. All attempts to obtain single crystals of complex **6** were unsuccessful.

2.2. Crystal Structures

The structures of complexes **1**–**5** have been determined by single-crystal X-ray diffraction. Table 1 collects selected bond lengths and angles of these complexes. Compounds **1**, **2**, **4** and **5** crystallize in the monoclinic C2/c space group and the cell unit includes, in all cases, four diruthenium units with no solvate molecules. However, complex **3** crystallizes in the orthorhombic Pbca space group with eight molecules in the cell unit and without solvent molecules.

The dimetallic units of complexes **1**–**5** consist of two Ru atoms linked by four amidate or carboxylate bridging ligands. Figures 1 and 2 show the dimetallic units of complexes **2** and **5**, respectively. The dimetallic unit of complexes **1**, **3** and **4** are collected in the Supplementary Material (Figures S1–S3). In all cases the axial positions are occupied by the halide ligand giving infinite zigzag

chains (Figures 3 and 4 for compounds **1** and **4**, respectively). Thus, each Ru atom shows a distorted octahedral environment having a RuN_2O_2 (amidates) and RuO_4 (carboxylates) environments in the equatorial positions and the axial sites occupied by one halide ligand and by the other Ru atom of the dimetallic unit.

Table 1. Selected bond lengths [Å] and angles [°] for compounds **1**–**5**.

	1	**2**	**3**	**4**	**5**
Distance (Å)					
Ru1-Ru1	2.2931(6)	2.2922(12)	-	2.2848(10)	2.2891(17)
Ru1-Ru2	-	-	2.2979(10)	-	-
Ru1-X	2.5875(6)	2.6909(9)	2.8623(10)	2.5631(11)	2.6027(19)
Ru2-X	-	-	2.8699(10)	-	-
Ru1 O1	2.035(3)	2.038(6)	2.053(6)	2.019(4)	2.016(7)
Ru1 O2	2.040(3)	2.029(6)	2.040(7)	2.013(4)	2.004(8)
Ru1-O3	-	-	2.045(6)	2.027(4)	2.031(7)
Ru1-O4	-	-	2.042(7)	2.022(4)	2.028(8)
Ru1-N1	2.047(3)	2.023(6)	2.033(6)	-	-
Ru1-N2	2.030(3)	2.024(6)	2.024(7)	-	-
Ru2-N3	-	-	2.013(6)	-	-
Ru2-N4	-	-	2.031(8)	-	-
Angles (º)					
Ru1-X-Ru1	124.51(5)	119.24(5)	-	124.89(8)	123.45(15)
Ru1-X-Ru2	-	-	101.84(3)	-	-
Ru1-Ru1-X	179.47(2)	178.29(5)	-	176.70(3)	176.60(7)
Ru1-Ru2-X	-	-	171.97(4)	-	-
Ru2-Ru1-X	-	-	175.71(4)	-	-
Torsion angles (º)					
O1-Ru1-Ru1-N1	−0.76	−0.13	−2.61/−1.44 [a]	-	-
O2-Ru1-Ru1-N2	−0.19	+0.99	−1.97/−3.02 [b]	-	-
O1-Ru1-Ru1-O4	-	-	-	−0.68	-
O2-Ru1-Ru1-O3	-	-	-	−0.99	-
O1-Ru1-Ru1-O3	-	-	-	-	−0.76
O2-Ru1-Ru1-O4	-	-	-	-	−0.59
θ angle/°	12.05 24.18	10.37 21.39	6.74 43.56	9.41 19.03	8.92 18.71

[a] O1-Ru1-Ru2-N4/O2-Ru1-Ru2-N3; [b] O3-Ru2-Ru1-N2/O4-Ru2-Ru1-N1.

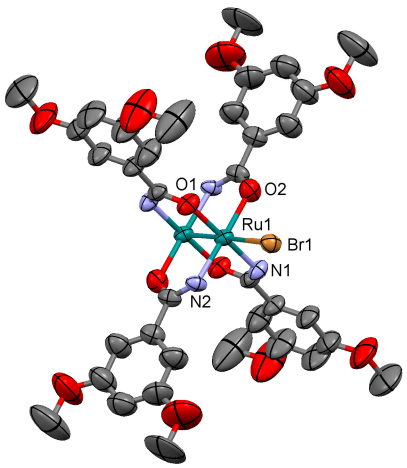

Figure 1. Representation of the dimeric unit in the structure of $[Ru_2Br(\mu\text{-}HNOCC_6H_3\text{-}3,5\text{-}(OMe)_2)_4]_n$ (**2**). Ellipsoids are drawn at 50% probability level. Hydrogen atoms are omitted for clarity.

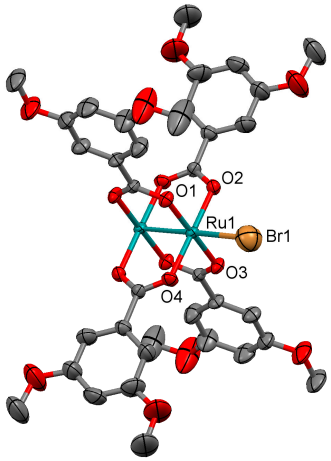

Figure 2. Representation of the dimeric unit in the structure of $[Ru_2Br(\mu\text{-}O_2CC_6H_3\text{-}3,5\text{-}(OMe)_2)_4]_n$ (**5**). Ellipsoids are drawn at 50% probability level. Hydrogen atoms are omitted for clarity.

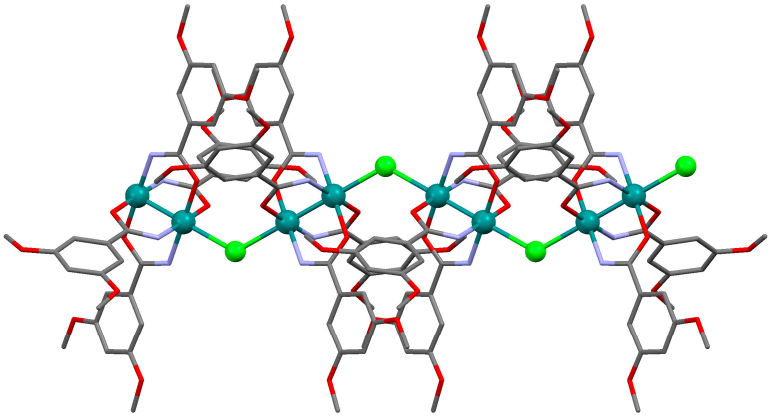

Figure 3. Drawing of a zigzag chain of $[Ru_2Cl(\mu\text{-}HNOCC_6H_3\text{-}3,5\text{-}(OMe)_2)_4]_n$ (**1**). Hydrogen atoms are omitted for clarity.

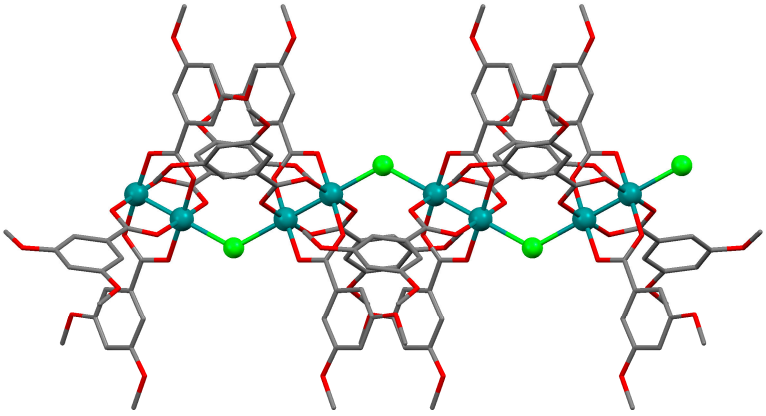

Figure 4. Drawing of a zigzag chain of $[Ru_2Cl(\mu\text{-}O_2CC_6H_3\text{-}3,5\text{-}(OMe)_2)_4]_n$ (**4**). Hydrogen atoms are omitted for clarity.

In the **1**–**3** amidate complexes, due to the asymmetry of the amidate ligands, four linkage isomers are possible, depending on the relative coordination of the ligands [17]. However, the three complexes show a *cis*-RuN_2O_2 environment similar to that observed in the other tetraamidatodiruthenium

complexes described in the literature [8,9,11–13,17,18]. Thus, in these complexes, each diruthenium unit resides on a center of inversion, and the asymmetric unit consists of two half dimers linked by the halide ligand, resulting in zigzag chains. Therefore, each diruthenium unit adopts a *cis*-RuN_2O_2 arrangement required by the inversion symmetry. Moreover, only two amidate complexes described in the literature [17,18] have a *trans*-RuN_2O_2 environment, but these complexes show a linear chain arrangement.

The Ru-Ru distances in the amidate complexes are slightly longer [2.2931(6) Å (1), 2.2922(12) Å (2), 2.2979(10) Å (3)] than the observed for carboxylate complexes [2.2848(10) Å (4), 2.2891(17) Å (5)] (Table 1). The higher donor character of the amidate ligands with respect to the carboxylate groups produces a higher electronic density on the ruthenium atoms giving a larger Ru-Ru distance. This is in accordance with the higher Ru-Ru distance found in the $[Ru_2(\mu\text{-N-N})_4]Cl$ compounds where N-N = formamidinate [20–23]. There are not significant differences in these distances with the change of the nature of the halide axial ligand. Obviously, the axial Ru-X distance increases from 2.5875(6) (**1**) to 2.8699(10) (**3**) when the halide ligand changes from chloride to iodide. The same behavior is observed in the carboxylate complexes **4** and **5**.

In the **1**–**3** amidate complexes, the Ru-X-Ru angle (Table 1) slightly decreases from the chloro [124.51(5)°] to the bromo derivative [119.24(5)°], although this decrease is more intense in the iodo derivative [101.84(3)°]. This variation has been attributed to the increase of the atomic volume of the halide ligand which determines a longer distance between the dimer units allowing the decrease of the Ru-X-Ru angle [18]. Similarly, in the carboxylate compounds **4** and **5**, this angle is slightly acute in the bromo derivative. In all cases, the zigzag chains are parallel to each other in the crystal and each chain is surrounded by another six chains. The zigzag chains are packed only by normal van der Waals forces. The centroid–centroid distances between phenyl rings are always larger than 3.8 Å and therefore the π-π stacking has not any effect on the packing of the chains [24]. Figure 5 shows the packing of the chains in complex **3**.

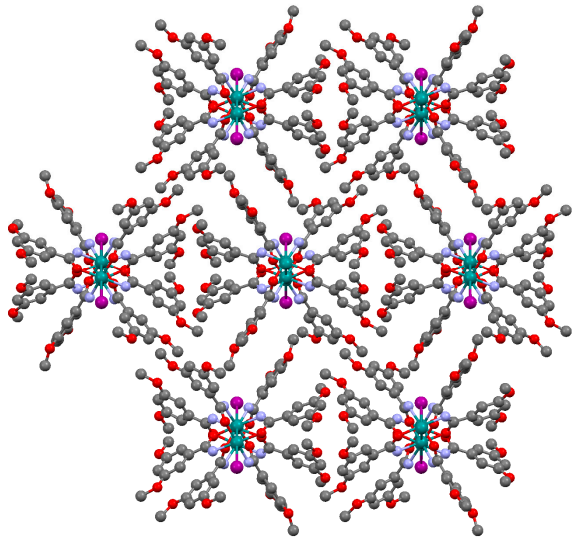

Figure 5. Packing of the zigzag chains in compound $[Ru_2I(\mu\text{-}HNOCC_6H_3\text{-}3,5\text{-}(OMe)_2)_4]_n$ (**3**). Hydrogen atoms are omitted for clarity.

In all cases the torsion angles O-Ru-Ru-N (**1**–**3**) and O-Ru-Ru-O (**4**, **5**) are very small, suggesting the absence of significant repulsions in the dimetallic units giving an almost eclipsed arrangement.

In these structures, the dihedral angle, θ, can be considered as the angle defined by the plane occupied by the carboxylate group and the ruthenium atoms and the plane defined by the phenyl ring (Table 1, Scheme 1).

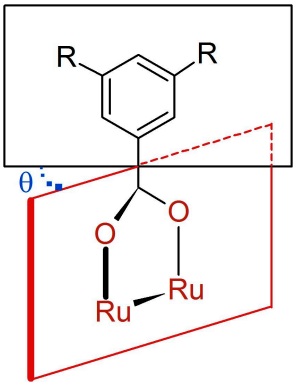

Scheme 1. Representation of the θ angle formed by the $Ru_2(\mu\text{-}O_2C)$ plane and the plane defined by the phenyl ring.

In complexes **1**–**5**, two θ angles are found, displaying a different orientation of the phenyl rings located in cis positions. A very similar rotation θ angle was found in the complexes **1**, **2**, **4** and **5** (Table 1), which indicates a low influence when the amidate ligand is changed by carboxylate ligands. However, in the iodo complex **3** one θ angle (43.56) is larger than in the rest of compounds (from 18.71 to 24.18). This fact, together with the presence of the iodide ligand, could determine the packing in the solid state since this complex crystallizes in the orthorhombic Pbca space group instead of in the C2/c space observed in the other complexes described in this work. Unfortunately, it has not been possible to obtain single crystals of the iodo complex **6** to compare the results. Figure 6 shows the θ angles observed in complex **3**.

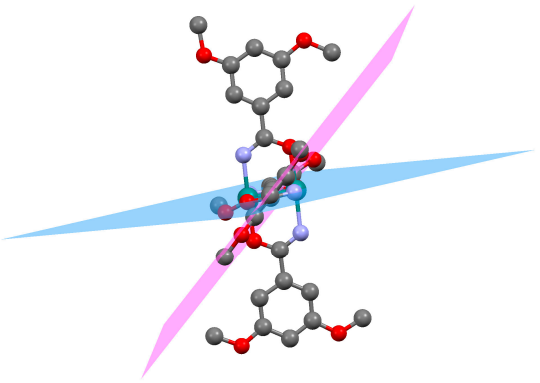

Figure 6. Torsion angle (θ) formed by the phenyl ring (pink plane) respect to the plane of the $Ru_2(\mu\text{-}O_2C)$ group (blue plane) in a dimetallic unit of complex $[Ru_2I(\mu\text{-}HNOCC_6H_3\text{-}3,5\text{-}(OMe)_2)_4]_n$ (**3**).

2.3. Spectroscopic Properties

The IR spectra of compounds **1**–**6** are very similar. The main differences between the IR spectra of the amidato (**1**–**3**) and carboxylato (**4**–**6**) complexes are (i) the presence in the amidato derivatives of a band at *ca.* 3350 cm^{-1} due to the NH stretching vibration and (ii) the strong bands observed in the 1500–1300 cm^{-1} region. In this region, the amidate complexes show a set of bands due to a combination of the ν(C=O) vibration (amide-I) and a mixture of the NH bending and ν(C-N) and ν(C-C) vibrations (amide-II) (Table 2). These bands are shifted to low frequencies with respect to the free amidate ligands. Complexes **4** and **5** show in this region strong bands due to the $\nu(COO)_s$ and $\nu(COO)_a$ stretching vibrations (Table 2).

Table 2. Selected bands in the IR spectra for compounds **1**–**6**.

Compound	Amide-I/Amide-II (cm^{-1})	$\nu(COO^-)_a$ (cm^{-1})	$\nu(COO^-)_s$ (cm^{-1})
1	1483, 1452, 1420	-	-
2	1483, 1451, 1420	-	-
3	1482, 1453, 1417	-	-
4	-	1448	1381
5	-	1449	1383
6		1449	1380

The UV-Vis-NIR spectra of compounds **1**–**6** show three main bands (Table 3). The bands observed in the range 321–346 nm are assigned to a charge transfer ligand-metal of the type σ(axial ligand) → σ*(Ru_2). The most characteristic bands observed in diruthenium complexes in the ranges 467–500 and 995–1153 nm are assigned to π(RuO/N,Ru_2) → π*(Ru_2) and δ(Ru_2) → δ*(Ru_2) according to previous studies [17,18,25,26].

Table 3. Selected bands in the UV-Vis-NIR spectra for compounds **1**–**6**.

Compound	σ(axial ligand) → σ*(Ru_2)	π(RuO/N,Ru_2) → π*(Ru_2)	δ(Ru_2) → δ*(Ru_2)
1	338	473	995
2	343	467	999
3	324	[a]	1002
4	321	482	1153
5	322	494	1137
6	346	500	1100

[a] Not clearly observed.

2.4. Magnetic Properties

The magnetic moments at room temperature of complexes **1**–**6** are in the range of 4.04 to 4.68 μ_B. These values are in accordance with the presence of three unpaired electrons per dimer unit in a ground-state configuration $\sigma^2\pi^4\delta^2(\pi^*\delta^*)^3$. This configuration was proposed by Norman and col. [27] as the basis for theoretical studies. In all complexes the molar magnetic susceptibility increases with decreasing temperature. However, the magnetic moment slowly decreases until about 100 K and then strongly decreases until 2 K. This behavior can be ascribed to the existence, in these type of complexes, of a strong zero-field splitting (ZFS), typical in diruthenium compounds, together with a non-negligible antiferromagnetic coupling between the dimetallic units mediated by the halide ligands or through-space.

The zero-field splitting effect on the susceptibility can be quantified by considering the Hamiltonian $H_D = S \times D \times S$, as described by O'Connor [28] which leads to the equation,

$$\chi_M = (\chi_{\parallel} + 2\chi_{\perp})/3$$

where

$$\chi_{\parallel} = (Ng^2\beta^2/kT)\,(1 + 9e^{-2D/kT})/4(1 + e^{-2D/kT})$$

$$\chi_{\perp} = (Ng^2\beta^2/kT)\,[4 + (3kT/D)(1 - e^{-2D/kT})]/4(1 + e^{-2D/kT})$$

The temperature independent paramagnetism (*TIP*) has been also introduced giving,

$$\chi'_M = \chi_M + TIP$$

The antiferromagnetic coupling has been considered as a perturbation by using the molecular field approximation [28],

$$\chi' = \chi'_M/[1 - (2zJ/Ng^2\beta^2)\,\chi'M]$$

Finally, the consideration of a paramagnetic impurity (P) leads to the final equation,

$$\chi'_{mol} = [(1 - P)\,\chi'] + [P\,Ng_{mo}{}^2\beta^2/4kT]$$

In these equations, the parameters N, g, zJ, k and D have the usual meanings. Using this model, a good agreement between the experimental and calculated curves of the molar susceptibility and the magnetic moment was obtained. Figure 7, shows the experimental and calculated curves for complex **1**. Similar curves have been obtained for complexes **2**–**6** (Figures S4–S8 in the Supplementary Material. The magnetic parameters (g, zJ, D, TIP, P and σ^2) obtained in the fits of the magnetic data of complexes **1**–**6** are collected in Table 4.

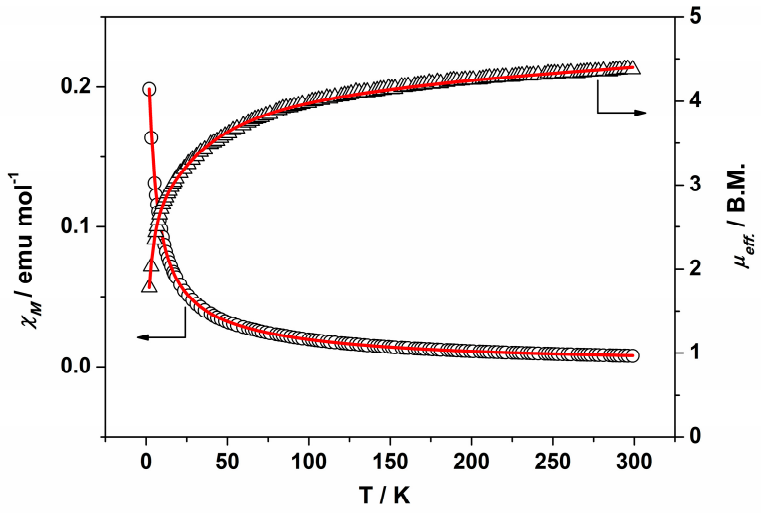

Figure 7. Temperature dependence of the molar magnetic susceptibility χ_M (circles) and μ_{eff} (triangles) for complex $[Ru_2Cl(\mu\text{-}HNOCC_6H_3\text{-}3,5\text{-}(OMe)_2)_4]_n$ (**1**); solid lines are the product of a least squares fit to the model indicated in the text.

Table 4. Magnetic parameters for compounds **1**–**6**.

	1	**2**	**3**	**4**	**5**	**6**
g	2.12	2.15	2.14	2.11	2.25	2.34
D (cm^{-1})	49.43	49.43	58.89	49.47	58.84	58.87
zJ (cm^{-1})	−2.05	−0.95	−3.62	−1.74	−2.29	−1.79
TIP (cm^3·mol^{-1})	1.3×10^{-3}	4.1×10^{-4}	1.9×10^{-7}	1.3×10^{-4}	7.4×10^{-4}	7.7×10^{-4}
P (%)	0.02	6.8×10^{-5}	0.04	4.1×10^{-5}	0.03	0.01
[a] σ^2	1.1×10^{-5}	2.9×10^{-5}	4.5×10^{-5}	4.0×10^{-5}	4.8×10^{-5}	2.6×10^{-5}

[a] $\sigma^2 = \Sigma(\mu_{eff\ calcd} - \mu_{eff\ exp})^2/\Sigma\mu_{eff\ exp}{}^2$.

There are no appreciable differences between the magnetic data of the amidate and carboxylates derivatives. The D values, ranging from 49.43 to 58.89 cm^{-1}, are similar to those found for analogous diruthenium complexes [3,17,18,29,30]. The low zJ values, from −0.95 to −3.62 cm^{-1}, are in accordance with a weak antiferromagnetic interaction between the dimetallic units mediated by the halide ligands in a zigzag chain [3,18]. The low Ru-X-Ru angles (from 101.84° to 124.89°) prevent a good orbital overlap between the diruthenium units and the halide ions, leading to the weak antiferromagnetic coupling. These values are lower than that observed in other diruthenium compounds which give linear chains, in the solid state, where the electronic communication is more favored [3,17,18,29]. Although a linear correlation between the strength of the magnetic coupling and the Ru–X/Ru–X–Ru ratio has been established [18,31] compound **2** does not correlate well because the zJ is the lowest of the five compounds. However, this fact is not unusual because the magnetic coupling value and the

Ru-X distance and the Ru-X-Ru angle depend on many factors and many other complexes are far from linearity.

3. Materials and Methods

3.1. General Aspects

All reactants and solvents were used as received. The precursors $[Ru_2X(\mu\text{-}O_2CMe)_4]$ (X = Cl, Br, I) were synthesized according to a published procedure [32–34].

Microwave reaction was carried out in an ETHOS ONE microwave oven using TFM Teflon closed vessels equipped with temperature sensor and pressure control. Solvothermal synthesis was carried out in a Memmert Universal Oven UFE 400 using Teflon-lined stainless steel autoclaves.

Elemental analyses were done by the Microanalytical Service of the Universidad Complutense de Madrid. FT-IR spectra were recorded in a Perkin Elmer Spectrum 100 with a universal ATR accessory with a spectral range of 4000–650 cm^{-1}. Electronic spectra of the complexes in the solid state were acquired on a Cary 5G spectrophotometer equipped with a Praying Mantis accessory for diffuse reflectance measurements. The reflectance data were converted by the instrument software to the F(R∞) values according to the Kubelka–Munk function. Magnetization measurements at variable temperature were obtained with a Quantum Design MPMSXL SQUID (Superconducting Quantum Interference Device) magnetometer over a temperature range of 2–300 K at the constant field of 1 T. Molar susceptibility values calculated from magnetization data were corrected for the diamagnetic contribution of both the sample holder and the compound to the susceptibility. The molar diamagnetic corrections for the complexes were calculated on the basis of Pascal's constants. Crushed crystals were used in the magnetic measurements to ensure the homogeneity of the sample.

3.2. Synthesis of Complexes

3.2.1. Synthesis of $[Ru_2Cl(\mu\text{-}NHOCC_6H_3\text{-}3,5\text{-}(OMe)_2)_4]_n$ (**1**)

Microwave assisted synthesis (method a). Chloridotetrakis(acetato)diruthenium(II,III) (0.12 g, 0.25 mmol), 3,5-dimethoxybenzamide (0.27 g, 1.50 mmol), lithium chloride (0.08 g, 2 mmol), triethylamine (0.25 mL) and absolute ethanol (8 mL) were added into a 85 mL TFM Teflon vessel with magnetic stirrer bar. The vessel was sealed with a lid equipped with temperature and pressure sensors and placed in the microwave oven. Reaction mixture was then treated by a three-step program consisting of (i) 15 min heating ramp up to 130 °C; (ii) 16 h isotherm at 130 °C; and (iii) 20 min cooling ramp up to room temperature. A brown suspension was obtained. The solid was obtained by filtration and washed twice with 10 mL of cold ethanol. Yield: 52%. Anal. Calcd. for $Ru_2ClC_{36}H_{43}N_4O_{13.5}$ (**1**·1.5H_2O): %C 43.88; %H 4.40; %N 5.69. Found: %C 43.57; %H 4.09; %N 5.61.

Solvothermal synthesis (method b). MeOH was used as solvent. Same reagents and quantities used in method (a) were added to a 23 mL Teflon-lined autoclave and stirred several minutes to become homogenised. The reactor was closed and heated under a three-step program consisting of (i) 2 h heating ramp up to 130 °C; (ii) 24 h isotherm at 130 °C; and (iii) 24 h cooling ramp up to room temperature. The microcrystalline brown solid obtained was filtered and washed with cold ethanol (2 × 10 mL). Yield: 62%. Anal. Calcd. for $Ru_2ClC_{36}H_{46}N_4O_{15}$ (**1**·3H_2O): %C 42.71; %H 4.58; %N 5.53. Found: %C 42.52; %H 4.14; %N 5.48.

IR (cm^{-1}): 3325w, 3017w, 2937w, 2833w, 1595m, 1509m, 1483w, 1452m, 1420m, 1343w, 1315m, 1300m, 1202m, 1180s, 1102w, 1046s, 942w, 921w, 851w, 919m, 756w, 744s, 686m. UV-Vis-NIR (diffuse reflection): [λ, nm] 338, 379, 473, 995. μ_{eff} (rt): 4.37 μ_B.

3.2.2. Synthesis of $[Ru_2Br(\mu\text{-}NHOCC_6H_3\text{-}3,5\text{-}(OMe)_2)_4]_n$ (**2**)

Microwave assisted synthesis (method a). Bromidotetrakis(acetato)diruthenium(II,III) (0.13 g, 0.25 mmol), 3,5-dimethoxybenzamide (0.27 g, 1.50 mmol), potassium bromide (0.24 g, 2 mmol),

triethylamine (0.25 mL) and absolute ethanol (8 mL) were added into a 85 mL TFM Teflon vessel with magnetic stirrer bar. The vessel was sealed with a lid equipped with temperature and pressure sensors, and placed in the microwave oven. Reaction mixture was then treated by a three-step program consisting of (i) 15 min heating ramp up to 120 °C; (ii) 16 h isotherm at 120 °C; and (iii) 20 min cooling ramp up to room temperature. A brown suspension was obtained. Solid is obtained by filtration and washed twice with 10 mL of cold ethanol and with 10 mL of water. Yield: 2%.

Solvothermal synthesis (method b). Same reagents and quantities used in method (a) were added to a 23 mL Teflon-lined autoclave and stirred several minutes to become homogenised. The reactor was closed and heated under a three-step program consisting of (i) 2 h heating ramp up to 100 °C; (ii) 24 h isotherm at 100 °C; and (iii) 48 h cooling ramp up to room temperature. The microcrystalline brown solid obtained was filtered and washed with cold ethanol (2 × 10 mL) and water (2 × 10 mL). Yield: 40%.

Anal. Calcd. for $Ru_2BrC_{36}H_{44}N_4O_{14}$ (**2**·$2H_2O$): %C 41.62; %H 4.27; %N 5.39. Found: %C 40.37; %H 3.59; %N 5.61. IR (cm^{-1}): 3321w, 3003w, 2930w, 2832w, 1596s, 1509s, 1483m, 1451s, 1420s, 1342m, 1316s, 1300s, 1285w, 1202s, 1172m, 1152s, 1101m, 1052s, 1047s, 944m, 922w, 862w, 851m, 819w, 755m, 744s, 686m. UV-Vis-NIR (diffuse reflection): [λ, nm] 343, 364, 467, 999. μ_{eff} (rt): 4.21 μ_B.

3.2.3. Synthesis of $[Ru_2I(\mu\text{-}NHOCC_6H_3\text{-}3,5\text{-}(OMe)_2)_4]_n$ (**3**)

Microwave assisted synthesis (method a). Iodotetrakis(acetato)diruthenium(II,III) (0.14 g, 0.25 mmol), 3,5-dimethoxybenzamide (0.27 g, 1.50 mmol), potassium iodide (0.34 g, 2 mmol), triethylamine (0.25 mL) and absolute ethanol (8 mL) were added into a 85 mL TFM Teflon vessel with magnetic stirrer bar. The vessel was sealed with a lid equipped with temperature and pressure sensors, and placed in the microwave oven. Reaction mixture was then treated by a three-step program consisting of (i) 15 min heating ramp up to 100 °C; (ii) 16 h isotherm at 100 °C; and (iii) 20 min cooling ramp up to room temperature. A brown suspension was obtained. Solid is obtained by filtration and washed twice with 10 mL of cold ethanol and with 10 mL of water. Yield: 48%. Anal. Calcd. for $Ru_2IC_{36}H_{44}N_4O_{14}$ (**3**·$2H_2O$): %C 39.82; %H 4.08; %N 5.16. Found: %C 39.60; %H 3.81; %N 5.05.

Solvothermal synthesis (method b). Same reagents and quantities used in method (a) were added to a 23 mL Teflon-lined autoclave and stirred several minutes to become homogenised. The reactor was closed and heated under a three-step program consisting of (i) 2 h heating ramp up to 100 °C; (ii) 24 h isotherm at 100 °C; and (iii) 48 h cooling ramp up to room temperature. The microcrystalline brown solid obtained was filtered and washed with cold ethanol (2 × 10 mL) and water (2 × 10 mL). Yield: 35%. Anal. Calcd. for $Ru_2IC_{36}H_{44}N_4O_{14}$ (**3**·$2H_2O$): %C 39.82; %H 4.08; %N 5.16. Found: %C 39.65; %H 3.94; %N 5.20.

IR (cm^{-1}): 3299w, 2997w, 2935w, 2835w, 1707w, 1595s, 1508s, 1482m, 1453s, 1417s, 1343m, 1315m 1297m, 1257w, 1202s, 1155s, 1112m, 1062s, 1049s, 992w, 940w, 923w, 841m, 756s, 743s, 689w. UV-Vis-NIR (diffuse reflection): [λ, nm] 324, 1002. μ_{eff} (rt): 4.04 μ_B.

3.2.4. Synthesis of $[Ru_2Cl(\mu\text{-}O_2CC_6H_3\text{-}3,5\text{-}(OMe)_2)_4]_n$ (**4**)

Microwave assisted synthesis (method a). Chloridotetrakis(acetato)diruthenium(II,III) (0.12 g, 0.25 mmol), 3,5-dimethoxybenzoic acid (0.27 g, 1.50 mmol) and methanol (8 mL) were added into a 85 mL TFM Teflon vessel with magnetic stirrer bar. The vessel was sealed with a lid equipped with temperature and pressure sensors, and placed in the microwave oven. Reaction mixture was then treated by a three-step program consisting of (i) 15 min heating ramp up to 130 °C; (ii) 16 h isotherm at 130 °C; and (iii) 20 min cooling ramp up to room temperature. A brown suspension was obtained. Solid is obtained by filtration and washed twice with 10 mL of cold methanol. Yield: 83%. Anal. Calcd. for $Ru_2ClC_{36}H_{40}O_{18}$ (**4**·$2H_2O$): %C 43.31; %H 4.04. Found: %C 43.34; %H 3.69.

Solvothermal synthesis (method b). Same reagents and quantities used in method (a) were added to a 23 mL Teflon-lined autoclave and stirred several minutes to become homogenised. The reactor was closed and heated under a three-step program consisting of (i) 2 h heating ramp up to 85 °C; (ii) 24 h

isotherm at 85 °C; and (iii) 72 h cooling ramp up to room temperature. The microcrystalline brown solid obtained was filtered and washed with cold methanol (2 × 10 mL). Yield: 90%. Anal. Calcd. for $Ru_2ClC_{36}H_{42}O_{19}$ (**4**·$3H_2O$): %C 42.55; %H 4.17. Found: %C 42.33; %H 3.64.

Conventional synthesis (method c). 0.27 g of 3,5-dimethoxybenzoic acid (1.50 mmol) were added to a suspension of chloridotetrakis(acetato)diruthenium(II,III) (0.12 g, 0.25 mmol) in 24 mL of MeOH/H_2O (1:1). The reaction mixture was refluxed for 4 h, yielding a brown precipitate. The solvent was eliminated by filtration and the brown solid was washed twice with 10 mL of cold methanol. Yield: 82%. Anal. Calcd. for $Ru_2ClC_{36}H_{40}O_{18}$ (**4**·$2H_2O$): %C 43.31; %H 4.04. Found: %C 43.07; %H 3.70.

IR (cm^{-1}): 3094w, 3003w, 2957w, 2937w, 2840w, 1593m, 1520w, 1481m, 1448m, 1433m, 1381s, 1312w, 1296w, 1251w, 1201m, 1157m, 1107w, 1058m, 1045m, 991w, 943m, 926w, 873w, 853w, 827w, 773m, 759s, 696w, 675w. UV-Vis-NIR (diffuse reflection): [λ, nm] 321, 482, 1153. μ_{eff} (rt): 4.04 μ_B.

3.2.5. Synthesis of $[Ru_2Br(\mu\text{-}O_2CC_6H_3\text{-}3,5\text{-}(OMe)_2)_4]_n$ (**5**)

Microwave assisted synthesis (method a). Bromidotetrakis(acetato)diruthenium(II,III) (0.13 g, 0.25 mmol), 3,5-dimethoxybenzoic acid (0.27 g, 1.50 mmol) and methanol (8 mL) were added into a 85 mL TFM Teflon vessel with magnetic stirrer bar. The vessel was sealed with a lid equipped with temperature and pressure sensors, and placed in the microwave oven. Reaction mixture was then treated by a three-step program consisting of (i) 15 min heating ramp up to 130 °C; (ii) 16 h isotherm at 130 °C; and (iii) 20 min cooling ramp up to room temperature. A brown suspension was obtained. Solid is obtained by filtration and washed twice with 10 mL of cold methanol. Yield: 84%. Anal. Calcd. for $Ru_2BrC_{36}H_{38}O_{17}$ (**5**·H_2O): %C 42.20; %H 3.74. Found: %C 42.19; %H 3.54.

Solvothermal synthesis (method b). Same reagents and quantities used in method (a) were added to a 23 mL Teflon-lined autoclave and stirred several minutes to become homogenised. The reactor was closed and heated under a three-step program consisting of (i) 2 h heating ramp up to 85 °C; (ii) 24 h isotherm at 85 °C; and (iii) 72 h cooling ramp up to room temperature. The microcrystalline brown solid obtained was filtered and washed with cold methanol (2 × 10 mL). Yield: 76%. Anal. Calcd. for $Ru_2BrC_{36}H_{36}O_{16}$ (**5**): %C 42.95; %H 3.60. Found: %C 43.30; %H 3.69.

Conventional synthesis (method c). 0.27 g of 3,5-dimethoxybenzoic acid (1.50 mmol) were added to a suspension of bromidotetrakis(acetato)diruthenium(II,III) (0.13 g, 0.25 mmol) in 30 mL of MeOH/H_2O (1:1). The reaction mixture was refluxed for 4 h, yielding a brown precipitate. The solvent was eliminated by filtration and the brown solid was washed twice with 10 mL of cold methanol. Yield: 80%. Anal. Calcd. for $Ru_2BrC_{36}H_{39}O_{17.5}$ (**5**·$1.5H_2O$): %C 41.83; %H 3.80. Found: %C 41.49; %H 3.49.

IR (cm^{-1}): 3003w, 2957w, 2935w, 2840w, 1593m, 1481w, 1449m, 1434w, 1383s, 1312w, 1296w, 1249w, 1202m, 1158m, 1107m, 1059w, 1046w, 991w, 943m, 926w, 873w, 853m, 828w, 773w, 760m, 697w, 675w. UV-Vis-NIR (diffuse reflection): [λ, nm] 322, 494, 1137. μ_{eff} (rt): 4.48 μ_B.

3.2.6. Synthesis of $[Ru_2I(\mu\text{-}O_2CC_6H_3\text{-}3,5\text{-}(OMe)_2)_4]_n$ (**6**)

Microwave assisted synthesis (method a). Iodotetrakis(acetato)diruthenium(II,III) (0.14 g, 0.25 mmol), 3,5-dimethoxybenzoic acid (0.27 g, 1.50 mmol) and methanol (8 mL) were added into a 85 mL TFM Teflon vessel with magnetic stirrer bar. The vessel was sealed with a lid equipped with temperature and pressure sensors, and placed in the microwave oven. Reaction mixture was then treated by a three-step program consisting of (i) 15 min heating ramp up to 130 °C; (ii) 16 h isotherm at 130 °C; and (iii) 20 min cooling ramp up to room temperature. A brown suspension was obtained. Solid is obtained by filtration and washed twice with 10 mL of cold ethanol. Yield: 71%. Anal. Calcd. for $Ru_2IC_{36}H_{42}O_{19}$ (**6**·$3H_2O$): %C 39.03; %H 3.82. Found: %C 38.74; %H 3.64.

Solvothermal synthesis (method b). Same reagents and quantities used in method (a) were added to a 23 mL Teflon-lined autoclave and stirred several minutes to become homogenised. The reactor was closed and heated under a three-step program consisting of (i) 2 h heating ramp up to 85 °C; (ii) 24 h isotherm at 85 °C; and (iii) 72 h cooling ramp up to room temperature. The microcrystalline brown

solid obtained was filtered and washed with cold ethanol (2 × 10 mL). Yield: 59%. Anal. Calcd. for $Ru_2IC_{36}H_{36}O_{16}$ (**6**): %C 41.04; %H 3.44. Found: %C 40.93; %H 3.59.

Conventional synthesis (method c). 0.27 g of 3,5-dimethoxybenzoic acid (1.50 mmol) were added to a suspension of iodotetrakis(acetato)diruthenium(II,III) (0.14 g, 0.25 mmol) in 30 mL of MeOH/H_2O (1:1). The reaction mixture was refluxed for 4 h, yielding a brown precipitate. The solvent was eliminated by filtration and the brown solid was washed twice with 10 mL of cold ethanol. Yield: 43%. Anal. Calcd. for $Ru_2IC_{36}H_{38}O_{17}$ (**6**·H_2O): %C 40.35; %H 3.57. Found: %C 39.01; %H 3.58.

IR (cm^{-1}): 3003w, 2938w, 2839w, 1596m, 1519w, 1481w, 1449m, 1380s, 1310w, 1290w, 1252w, 1204m, 1155s, 1110w, 1062m, 1048m, 1017m, 1002m, 945w, 925w, 873w, 845w, 827w, 792w, 760m, 698m, 673w. UV-Vis-NIR (diffuse reflection): [λ, nm] 346, 500, 1100. μ_{eff} (rt): 4.68 μ_B.

3.3. Crystal Structure Determination

Details of the data collection and crystal structure refinement for **1**–**5** are given in Tables 5 and 6.

Table 5. Crystal data and structure refinement for **1**–**3**.

Compound	1	2	3
Empirical formula	C36 H40 Cl N4 O12 Ru2	C36 H40 Br N4 O12 Ru2	C36 H40 I N4 O12 Ru2
Formula weight	958.31	1002.77	1049.76
Temperature	293(2) K	293(2) K	293(2) K
Wavelength	0.71073 Å	0.71073 Å	0.71073 Å
Crystal system	Monoclinic	Monoclinic	Orthorhombic
Space group	C2/c	C2/c	Pbca
a	23.6020(5) Å	23.6552(16) Å	24.9352(11) Å
b	12.9621(2) Å	12.9492(9) Å	12.7509(5) Å
c	13.2114(3) Å	13.3075(9) Å	27.8809(15) Å
α	90°	90°	90°
β	111.009(2)°	111.0620(10)°	90°
γ	90°	90°	90°
Volume	3773.10(13) $Å^3$	3804.0(4) $Å^3$	8864.7(7) $Å^3$
Z	4	4	8
Density	1.687 Mg/m^3	1.751 Mg/m^3	1.573 Mg/m^3
Absorption coefficient	0.940 mm^{-1}	1.912 mm^{-1}	1.436 mm^{-1}
F(000)	1940	2012	4168
Crystal size	0.45 × 0.18 × 0.13 mm^3	0.23 × 0.12 × 0.10 mm^3	0.39 × 0.12 × 0.05 mm^3
Theta range for data collection	2.67° to 26.00°	1.82° to 26.00°	3.28° to 25.01°
Index ranges	$-9 \leq h \leq 25$ $-15 \leq k \leq 15$ $-16 \leq l \leq 15$	$-29 \leq h \leq 29$ $-14 \leq k \leq 15$ $-16 \leq l \leq 16$	$-29 \leq h \leq 21$ $-11 \leq k \leq 15$ $-33 \leq l \leq 25$
Reflections collected	14838	15382	26230
Independent reflections	3710 [R(int) = 0.0250]	3707 [R(int) = 0.0444]	7798 [R(int) = 0.0585]
Completeness to theta	99.9%	99.0%	99.8%
Absorption correction	None	None	Semi-empirical from equivalents
Refinement method	Full-matrix least squares on F^2	Full-matrix least squares on F^2	Full-matrix least squares on F^2
Data/restrains/parameters	3710/4/234	3707/8/189	7798/1/490
Goodness-of-fit on F^2	1.057	0.997	0.998
Final R indices [I > 2sigma(I)]	R1 = 0.0382 wR2 = 0.1059	R1 = 0.0547 wR2 = 0.1447	R1 = 0.0757 wR2 = 0.2118
R indices (all data)	R1 = 0.0464 wR2 = 0.1106	R1 = 0.0974 wR2 = 0.1897	R1 = 0.1280 wR2 = 0.2394
Largest diff. peak and hole	1.485 and −1.254 e $Å^{-3}$	1.286 and −0.715 e $Å^{-3}$	1.431 and −1.129 e $Å^{-3}$

$R(F) = \Sigma||F_0| - |F_c||/\Sigma|F_0|$. $wR(F_0)^2 = \{\Sigma[w(F_0^2 - F_c^2)^2]/\Sigma[w(F_0^2)^2]\}^{1/2}$.

Table 6. Crystal data and structure refinement for **4** and **5**.

Compound	4	5
Empirical formula	C36 H36 Cl O16 Ru2	C36 H36 Br O16 Ru2
Formula weight	962.24	1006.70
Temperature	293(2) K	293(2) K
Wavelength	0.71073 Å	0.71073 Å
Crystal system	Monoclinic	Monoclinic
Space group	C2/c	C2/c
a	23.187(3) Å	23.277(3) Å
b	12.8452(18) Å	12.8620(14) Å
c	13.1625(19) Å	13.2455(14) Å
α	90°	90°
β	110.379(2)°	110.633(2)°
γ	90°	90°
Volume	3675.0(9) $Å^3$	3711.2(7) $Å^3$
Z	4	4
Density	1.739 Mg/m^3	1.802 Mg/m^3
Absorption coefficient	0.970 mm^{-1}	1.966 mm^{-1}
F(000)	1940	2012
Crystal size	0.44 × 0.07 × 0.05 mm^3	0.44 × 0.09 × 0.07 mm^3
Theta range for data collection	1.84° to 25.00°	1.84° to 25.00°
Index ranges	$-27 \leq h \leq 27$ $-13 \leq k \leq 15$ $-15 \leq l \leq 15$	$-27 \leq h \leq 27$ $-15 \leq k \leq 12$ $-15 \leq l \leq 15$
Reflections collected	13717	13572
Independent reflections	3228 [R(int) = 0.0543]	3232 [R(int) = 0.0549]
Completeness to theta	99.4%	98.4%
Absorption correction	None	None
Refinement method	Full-matrix least squares on F^2	Full-matrix least squares on F^2
Data/restrains/parameters	3228/0/209	3232/0/225
Goodness-of-fit on F^2	0.998	0.999
Final R indices [I>2sigma(I)]	R1 = 0.0527 wR2 = 0.1476	R1 = 0.0781 wR2 = 0.2316
R indices (all data)	R1 = 0.0658 wR2 = 0.1564	R1 = 0.1080 wR2 = 0.2562
Largest diff. peak and hole	1.255 and −1.301 e $Å^{-3}$	1.427 and −4.062 e $Å^{-3}$

$R(F) = \Sigma||F_0| - |F_c||/\Sigma|F_0|$. $wR(F_0)^2 = \{\Sigma[w(F_0^2 - F_c^2)^2]/\Sigma[w(F_0^2)^2]\}^{1/2}$.

Data collection for **2**, **4** and **5** was carried out at room temperature on a Bruker Smart CCD diffractometer using graphite-monochromated Mo-Kα radiation (λ = 0.71073 Å) operating at 50 kV and 35 mA for **2** and **5**, and 50 kV and 30 mA for **4**. The data were collected over a hemisphere of the reciprocal space by combination of three exposure sets. Each exposure of 20 s covered 0.3 in ω. The cell parameters were determined and refined by a least-squares fit of all reflections. The first 100 frames were recollected at the end of the data collection to monitor crystal decay, and no appreciable decay was observed.

Data collection for **1** and **3** was carried out at room temperature on a Xcalibur-Atlas CCD diffractometer using graphite-monochromated Mo-Kα radiation (λ = 0.71073 Å) operating at 50 kV and 40 mA. The exposure time were 19.62 s and 75 s in ω respectively.

The structures were solved by direct methods and refined by full-matrix least-square procedures on F^2 (SHELXL-97) [35]. All non-hydrogen atoms were refined anisotropically. In complex **1**, C18 has been splitted in two positions to solve the disorder. All hydrogen atoms were included in their calculated positions and refined riding on the respective carbon atoms. Mercury CSD 3.9 [36] was used for molecular graphics.

CCDC 1556299-1556303 contains the supplementary crystallographic data for this paper. These data can be obtained free of charge from The Cambridge Crystallographic Data Centre via www.ccdc.cam.ac.uk/data_request/cif. This material is available free of charge via the Internet at http://pubs.acs.org.

4. Conclusions

Single crystals of complexes **1**–**5** were obtained using solvothermal procedures. Amidato and carboxylato complexes can also be prepared by microwave activation, but no single crystals can be obtained by this type of activation. Carboxylato complexes can be obtained using conventional methods, but only the solvothermal activation leads to the formation of single crystals. There are no significant differences in the properties of these compounds when the 3,5-dimethoxybenzamidate ligand is replaced by the 3,5-dimethoxybenzoate groups.

Supplementary Materials: The following are available online at www.mdpi.com/2073-4352/7/7/192/s1: Figures S1–S3: representation of the dimeric unit in the structure of complexes **1**, **3** and **4**. Figures S4–S8: Temperature dependence of the molar magnetic susceptibility χ_M (circles) and μ_{eff} (triangles) for complexes **2**–**6**; solid lines are the product of a least squares fit to the model indicated in the text.

Acknowledgments: Spanish Ministerio de Economía y Competitividad (CTQ2015-63858-P, MINECO/FEDER) is gratefully acknowledged.

Author Contributions: R.J.-A. and J.L.P. conceived and designed the experiments; P.D.-M. and C.F. performed the experiments; R.J.-A., J.L.P., R.G.-P., and P.D.-M. analyzed the data and wrote the paper. P.D.-M. and M.R.T. have carried out the crystal structure determination of the complexes.

Conflicts of Interest: The authors declare no conflict of interest.

References

1. Cotton, F.A.; Murillo, C.A.; Walton, R.A. *Multiple Bonds between Metal Atoms*, 3rd ed.; Springer: New York, NY, USA, 2005; pp. 377–430.
2. Aquino, M.A.S. Recent developments in the synthesis and properties of diruthenium tetracarboxylates. *Coord. Chem. Rev.* **2004**, *248*, 1025–1045. [CrossRef]
3. Mikuriya, M.; Yoshioka, D.; Handa, M. Magnetic interactions in one-, two-, and three-dimensional assemblies of dinuclear ruthenium carboxylates. *Coord. Chem. Rev.* **2006**, *250*, 2194–2211. [CrossRef]
4. Das, B.; Chakravarty, A.R. Synthesis and Physico-Chemical Properties of Diruthenium(III,II) Tetra-aryl Carboxylato Compounds. *Polyhedron* **1988**, *7*, 685–687. [CrossRef]
5. Barral, M.C.; Jiménez-Aparicio, R.; Rial, C.; Royer, E.C.; Saucedo, M.J.; Urbanos, F.A. Synthesis and Characterization of new Carboxylate Dimers of Ruthenium. *Polyhedron* **1990**, *9*, 1723–1728. [CrossRef]
6. Malinski, T.; Chang, D.; Feldmann, F.N.; Bear, J.L.; Kadish, K.M. Electrochemical Studies of a Novel Ruthenium(II,III) Dimer, $Ru_2(HNOCCF_3)_4Cl$. *Inorg. Chem.* **1983**, *22*, 3225–3233. [CrossRef]
7. Chavan, M.Y.; Feldmann, F.N.; Lin, X.Q.; Bear, J.L.; Kadish, K.M. Electrochemical Generation of New Dinuclear Ruthenium Acetamidate Complexes. *Inorg. Chem.* **1984**, *23*, 2373–3275. [CrossRef]
8. Chakravarty, A.R.; Cotton, F.A.; Tocher, D.A. Structure of a Diruthenum(II,III) Complex with Benzamidate Bridging Ligands. *Polyhedron* **1985**, *4*, 1957–1958. [CrossRef]
9. Chakravarty, A.R.; Cotton, F.A. Synthesis and Structure of a Binuclear ruthenium 4-Chlorobenzamidato Complex. *Polyhedron* **1985**, *4*, 1097–1102. [CrossRef]
10. Ryde, K.; Tocher, D.A. The Electra-oxidation of the Binuclear Ruthenium(II/III) Tetraamidate Complex, $Ru_2(Me_3CCONH)_4Cl$. *Inorg. Chim. Acta* **1986**, *118*, L49–L51. [CrossRef]
11. Barral, M.C.; Jiménez-Aparicio, R.; Monge, A.; Priego, J.L.; Royer, E.C.; Ruíz-Valero, C.; Urbanos, F.A. Tert-butylbenzamidatediruthenium(II,III) Compounds. Crystal Structure of $[Ru_2(\mu\text{-}HNOCC_6H_4\text{-}p\text{-}CMe_3)_4(OPPh_3)_2]BF_4$. *Polyhedron* **1993**, *12*, 2947–2953. [CrossRef]
12. Barral, M.C.; de la Fuente, I.; Jiménez-Aparicio, R.; Priego, J.L.; Torres, M.R.; Urbanos, F.A. Synthesis of diruthenium(II,III) amidate compounds. Crystal structure of $[Ru_2(\mu\text{-}HNOCC_4H_3S)_4(thf)_2]SbF_6 \cdot 0.5$cyclohexane. *Polyhedron* **2001**, *20*, 2537–2544. [CrossRef]
13. Villalobos, L.; Cao, Z.; Fanwick, P.E.; Ren, T. Diruthenium(II,III) tetramidates as a new class of oxygenation catalysts. *Dalton Trans.* **2012**, *41*, 644–650. [CrossRef] [PubMed]
14. Johnson, K.D.; Powell, G.L. Microwave-assisted synthesis of dimolybdenum tetracarboxylates and a decanuclear osmium cluster. *J. Organomet. Chem.* **2008**, *693*, 1712–1715. [CrossRef]
15. Herrero, S.; Jiménez-Aparicio, R.; Perles, J.; Priego, J.L.; Urbanos, F.A. First microwave synthesis of multiple metal-metal bond paddlewheel compounds. *Green Chem.* **2010**, *12*, 965–967. [CrossRef]

16. Herrero, S.; Jiménez-Aparicio, R.; Perles, J.; Priego, J.L.; Saguar, S.; Urbanos, F.A. Microwave methods for the synthesis of paddlewheel diruthenium compounds with N,N-donor ligands. *Green Chem.* **2011**, *13*, 1885–1890. [CrossRef]
17. Delgado, P.; González-Prieto, R.; Jiménez-Aparicio, R.; Perles, J.; Priego, J.L.; Torres, M.R. Comparative study of different methods for the preparation of tetraamidato and tetracarboxylatodiruthenium compounds. Structural and magnetic characterization. *Dalton Trans.* **2012**, *41*, 11866–11874. [CrossRef] [PubMed]
18. Delgado-Martínez, P.; Gómez-García, C.J.; González-Prieto, R.; Jiménez-Aparicio, R.; Priego, J.L.; Torres, M.R. Structural, magnetic and electrical properties of one-dimensional tetraamidatodiruthenium compounds. *Dalton Trans.* **2014**, *43*, 3227–3237. [CrossRef] [PubMed]
19. Lin, C.; Ren, T.; Valente, E.J.; Zubkowski, J.D.; Smith, E.T. Continuous Spectroscopy and Redox Tuning of Dinuclear Compounds: Chlorotetrakis(μ-N,N′-diarylformamidinato)diruthenium(II,III). *Chem. Lett.* **1997**, *26*, 753–754. [CrossRef]
20. Chiarella, G.N.; Cotton, F.A.; Murillo, C.A.; Ventura, K.; Villagrán, D.; Wang, X. Manipulating Magnetism: Ru_2^{5+} Paddlewheels Devoid of Axial Interactions. *J. Am. Chem. Soc.* **2014**, *136*, 9580–9589. [CrossRef] [PubMed]
21. Chen, W.-Z.; Fanwick, P.E.; Ren, T. Peripheral Functionalization of Diruthenium Compounds via Heck Reactions. *Organometallics* **2007**, *26*, 4115–4117. [CrossRef]
22. Xu, G.-L.; Ren, T. Suzuki Coupling at the Periphery of Diruthenium Coordination and Organometallic Compounds. *Inorg. Chem.* **2006**, *45*, 10449–10456. [CrossRef] [PubMed]
23. Bear, J.L.; Han, B.; Huang, S.; Kadish, K.M. Effect of Axial Ligands on the Oxidation State, Structure, and Electronic Configuration of Diruthenium Complexes. Synthesis and Characterization of $Ru_2(dpf)_4Cl$, $Ru_2(dpf)_4(C{\equiv}CC_6H_5)$, $Ru_2(dpf)_4(C{\equiv}CC_6H_5)_2$, and $Ru_2(dpf)_4(CN)_2$ (dpf = N,N′-Diphenylformamidinate). *Inorg. Chem.* **1996**, *35*, 3012–3021. [CrossRef]
24. Janiak, C. A critical account on π–π stacking in metal complexes with aromatic nitrogen-containing ligands. *J. Chem. Soc. Dalton Trans.* **2000**, *21*, 3885–3896. [CrossRef]
25. Miskowski, V.M.; Loehr, T.M.; Gray, H.B. Electronic and Vibrational Spectra of $Ru_2(carboxylate)_4^+$ Complexes. Characterization of a High-Spin Metal-Metal Ground State. *Inorg. Chem.* **1987**, *26*, 1098–1108. [CrossRef]
26. Miskowski, V.M.; Gray, H.B. Electronic Spectra of $Ru_2(carboxylate)_4^+$ Complexes. Higher Energy Electronic Excited States. *Inorg. Chem.* **1988**, *27*, 2501–2506. [CrossRef]
27. Norman, G.J.; Renzoni, G.E.; Case, D.A. Electronic Structure of $Ru_2(O_2CR)_4^+$ and $Rh_2(O_2CR)_4^+$ Complexes. *J. Am. Chem. Soc.* **1979**, *101*, 5256–5267. [CrossRef]
28. O'Connor, C.J. Magnetochemistry-Advances in Theory and Experimentation. *Prog. Inorg. Chem.* **1982**, *29*, 203–283.
29. Jiménez-Aparicio, R.; Urbanos, F.A.; Arrieta, J.M. Magnetic Properties of Diruthenium(II,III) Carboxylate Compounds with Large Zero-Field Splitting and Strong Antiferromagnetic Coupling. *Inorg. Chem.* **2001**, *40*, 613–619. [CrossRef] [PubMed]
30. Chen, W.-Z.; Cotton, F.A.; Dalal, N.S.; Murillo, C.A.; Ramsey, C.M.; Ren, T.; Wang, X. Proof of Large Positive Zero-Field Splitting in a Ru_2^{5+} Paddlewheel. *J. Am. Chem. Soc.* **2005**, *127*, 12691–12696. [CrossRef] [PubMed]
31. Estiú, G.; Cukiernik, F.D.; Maldivi, P.; Poizat, O. Electronic, Magnetic, and Spectroscopic Properties of Binuclear Diruthenium Tetracarboxylates: A Theoretical and Experimental Study. *Inorg. Chem.* **1999**, *38*, 3030–3039. [CrossRef]
32. Mitchell, R.W.; Spencer, A.; Wilkinson, G. Carboxylato-triphenylphosphine Complexes of Ruthenium, Cationic Triphenylphosphine Complexes derived from them, and their Behaviour as Homogeneous Hydrogenation Catalysts for Alkenes. *J. Chem. Soc. Dalton Trans.* **1973**, 846–854. [CrossRef]
33. Mukaida, M.; Nomura, T.; Ishimori, T. Syntheses of formato-, acetato-, benezoato-, and chloro-substituted acetatoruthenium complexes, and their properties. *Bull. Chem. Soc. Jpn.* **1972**, *45*, 2143–2147. [CrossRef]
34. González-Prieto, R. Compuestos Dinucleares de Rutenio: Propiedades, Tipos de Ordenamiento y Aplicaciones Como Materiales Moleculares. Ph.D. Thesis, University Complutense of Madrid, Madrid, Spain, 2005.

35. Siemens. *SMART, SAINT and SHELXTL*; Siemens Analytical X-ray Instruments Inc.: Madison, WI, USA, 1996.
36. Mercury, C.S.D.; Bruno, I.J.; Chisholm, J.A.; Edgington, P.R.; McCabe, P.; Pidcock, E.; Rodriguez-Monge, R.; Taylor, L.; Van de Streek, J.; Wood, P.A. Mercury CSD 2.0—New features for the visualization and investigation of crystal structures. *J. Appl. Crystallogr.* **2008**, *41*, 466–470.